Building and Environment 169 (2020) 106564

Contents lists available at ScienceDirect

Building and Environment

journal homepage: http://www.elsevier.com/locate/buildenv

The impact of building configurations and anthropogenic heat on daily urban air temperature cycles

Yu Xue [a], Yi Wang [b,c,*], Haiying Peng [a], Haidong Wang [d], Jin Shen [e]

[a] School of Civil Engineering, Dalian University of Technology, Linggong Road, Dalian, China
[b] Advanced Study Program, National Center for Atmospheric Research, Boulder, CO, USA
[c] Research Applications Laboratory, National Center for Atmospheric Research, Boulder, CO, USA
[d] School of Environment and Architecture, University of Shanghai for Science and Technology, 516 Jungong Road, Shanghai, China
[e] State Environmental Key Laboratory of Regional Air Quality Monitoring, Guangdong Environmental Protection Key Laboratory of Secondary Air Pollution Research, Guangdong Environmental Monitoring Center, Guangzhou, China

ARTICLE INFO

Keywords:
Diurnal urban air temperature
Lumped urban air temperature model
Urban morphology
Anthropogenic heat

ABSTRACT

Urban air temperature reflects the impact of urbanization on thermal and dynamics of urban climate. To understand the physical mechanism of building configurations and anthropogenic heat on daily urban air temperature cycles, an improved lumped urban air temperature model was provided. The surface energy balance equation for the improved and previous lumped urban air temperature model were compared. The effective depth of thermal mass and sub-surface temperature of urban surfaces in the previous model can be determined, which are usually chosen from model studies. These two parameters have a significant impact on the thermal storage. The models were evaluated and applied to the city of Hong Kong. Thermal storage is shown to have significant impact on the amplitude and phase term of daily air temperature cycle. Moreover, the building configurations can affect the solar radiation gain and redistribution in the sub-facets, which indirectly influenced the urban air temperature. The results show that the ventilation rate, building height and plan area ratio play important roles on daily cycle of urban air temperature, while the anthropogenic heat plays a less significant role. The main distinction of the improved model is its simplicity and less computation cost for practice use for engineers and urban planners. Two important parameters are emphasized, relative convective heat transfer number, λ, and time constant, τ. The two parameters provide some insights on how to control the urban thermal environment in an engineering way.

1. Introduction

Urbanization is one of the most evident effects of human development [1–3]. The UHI effect, in which the air temperatures in urban areas exceed those in the surrounding rural areas, has been extensively studied [2–5]. UHI is closely related to the urban morphology, including the building density, building height, sky view factor, urban classification, and spatial coverage of urban surfaces [6–12]. The air temperature in the urban canopy is highly variable and is closely related to the urban morphology [9]. The surface heterogeneity of urban areas resulting from the massive volumes of different buildings has been shown to be the main contributor to the UHI effect [11]. The heterogeneity of the building heights, building densities, and sky view factors results in increased absorption of solar radiation and reduced outgoing longwave radiation, which leads to higher street surface temperatures and indirectly influences the urban air temperature [11–13]. Anthropogenic heat also increases the sensible and latent heat fluxes within the urban canopy layer [2,13]. These factors have significant effects on the urban climate, which can be quantitatively understood in terms of the energy balance in the urban canopy layer.

The surface energy balance is considered to be fundamental to understanding the boundary layer meteorology and climatology of any site [2]. Coupled with the background wind, the surface energy provides the driving force for the vertical fluxes of heat, mass, and momentum [2]. Hence, it is important to examine the nature of the surface energy balance to understand the thermodynamic behavior of the air and the surface temperature, the dynamics of the local airflow and boundary layer depth, and the concentration of air pollutants [2,5–7]. In the past decades, many urban canopy models (UCM) have been developed for improving our theoretical understanding of the phenomenon. Mostly, these models focus on the surface energy transport and aerodynamics

* Corresponding author. Advanced Study Program, National Center for Atmospheric Research, Boulder, CO, USA.
E-mail addresses: yiyiwang@ucar.edu, yironnywang@gmail.com (Y. Wang).

https://doi.org/10.1016/j.buildenv.2019.106564
Received 9 October 2019; Received in revised form 19 November 2019; Accepted 20 November 2019
Available online 23 November 2019

List of symbols

A_p	plan area of urban areas, m^2
A_b	built area of urban areas, m^2
A_{ps}	urban street areas, m^2
A_{pr}	urban building roof areas, m^2
A_{pn}	urban natural surfaces areas, m^2
A_{bw}	building wall surfaces areas, m^2
f_s	proportion of urban street area to plan area
f_r	proportion of building roof area to plan area
f_n	proportion of natural surfaces area to plan area
f_w	proportion of building wall surfaces area to plan area
h	urban control volume height, m
q	ventilation rate, $m^3\ s^{-1}$
v	air velocity in the urban canopy layer, $m\ s^{-1}$
ρ	air density, $kg\ m^{-3}$
C_p	specific heat of air, $J\ K^{-1}\ kg^{-1}$
h_c	convection heat transfer coefficient, $W\ K^{-1}\ m^{-2}$
λ_p	conductive heat transfer coefficient, $W\ K^{-1}\ m^{-1}$
h_{rad}	longwave radiation heat transfer coefficient, $W\ K^{-1}\ m^{-2}$
F_{sky}	sky view factor
ε	emissivity of urban areas
α	urban albedo
ρ_s	density of urban surfaces, $kg\ m^{-3}$
C_s	specific heat of urban surfaces, $J\ K^{-1}\ kg^{-1}$
a_p	thermal diffusivity, $m^2\ s^{-1}$
m	mass of the urban materials, kg
Δz	distance between urban surface and the measured sub-surfaces, m
ρ_{H_2O}	water density, kgm^{-3}
E_t	measured hourly evaporation rate, $m\ s^{-1}$
L_v	latent heat of vaporization, $J\ kg^{-1}$
λ	relative convective heat transfer number
λ_{sky}	relative sky radiation number
λ_k	relative conductive heat transfer number
τ	time constant, s
d_j	penetration depth, m
d_{ej}	effective depth, m
T_r	rural air temperature, K
T_u	urban air temperature, K
T_s	urban surface temperature, K
T_m	sub-surface temperature of urban surfaces, K
Q_{anth}	anthropogenic heat flux, $W\ m^{-2}$
Q_{sol}	solar radiation heat flux, $W\ m^{-2}$
Q_{evp}	evaporation heat flux, $W\ m^{-2}$
Q_{conv}	convection heat flux, $W\ m^{-2}$
Q_{rad}	longwave radiation heat flux, $W\ m^{-2}$
$Q_{cond(0,t)}$	conduction heat flux at urban surface level, $W\ m^{-2}$

inside the urban canopy layer. The urban canopy models can be divided into two groups: the single layer canopy model which mainly focus on the surface temperatures and surface energy balance, and multilayer canopy model which mainly focus on the turbulence exchange beyond the building height level and atmospheric flow dynamics inside the boundary layer [14–17]. The urban canopy models are also incorporated with the existing mesoscale meteorological models, such as Weather Research and Forecasting (WRF) model to describe the response of atmosphere to urban surfaces [18].

The existing urban canopy models are not simple enough to link the urban air temperature to the urban morphology or urban characterization within the urban canopy layer in a quantitative way. Silva et al. [19] first introduced a zero-dimensional mesoscale thermal model for urban climate to allow the users to rapidly predict a characteristic urban temperature. However, the model result does not distinguish the urban air temperature from the urban surface temperature, which can be very different [5]. Therefore, Yang et al. [5] incorporated the energy balance between urban air and urban surfaces while retaining the simplicity of the model. However, Yang et al. [5] estimated the effective depth of thermal mass and sub-surface temperature of urban surfaces in the surface energy equation. These two parameters have a significant impact on the thermal storage, and the amplitude and phase term of daily air temperature cycle. This study is a step forward from Yang et al. [5] to study the impact of building configurations and anthropogenic heat on daily urban air temperature cycles. The effective depth of ground or walls is introduced in the city surface energy balance equation. Therefore, the uncertain value of effective depth of thermal mass and sub-surface temperature of urban surfaces in Yang et al. [5] can be determined.

In this study, the previous lumped urban air temperature model developed by Yang et al. [5] and the improved model are illustrated and compared. The model is tested and evaluated in the city of Hong Kong. The outcomes of the improved model are to understand the physical mechanisms of the diurnal cycle of urban air temperature and to provide quantitative understanding of impact of building configurations and anthropogenic heat on urban thermal environment. Moreover, the results of this study could provide some insights on design of urban building configurations for a climate-resilient city.

2. Methodology

2.1. Previous lumped urban air temperature model introduced by Yang et al. [5]

An effective way to describe the urban energy balance is to replace the concept of a massless surface plane or interface with that of a near-surface active layer or volume [2,20]. This approach ignores the exact nature of the surface, including the spatial diversity and vertical unevenness, and treats it as an integrated system [20]. Fig. 1 introduces the energy exchange between the urban surface and atmosphere in an idealized urban area. In this model, average building height, which is the same as the widely used single-layer urban canopy model [17,19,21], and simplified whole complex urban fabrics to four different types, building roofs, building walls, urban streets, and natural surfaces, are used for representing the real configurations. The plan area, A_p, and total building surface area, A_b, are then illustrated by the following equation:

$$A_p = A_{ps} + A_{pr} + A_{pn} = (f_s + f_r + f_n)A_p \quad (1)$$

$$A_b = A_p + A_{bw} = (1 + f_w)A_p \quad (2)$$

where f_w is the ratio of building surface area to unit ground area.

For the ideal urban model, the urban air is assumed to be well mixed and the air temperature as uniform within the urban canopy layer (shown in Fig. 1). As such, the city air energy balance is:

$$\rho C_p q(T_r - T_u) + h_c(T_s - T_u)A_b + A_p Q_{anth} = 0 \quad (3)$$

where the first term is the net advection from rural to urban areas; the second term is the convective heat transfer between urban surfaces and atmosphere; and the last term is the anthropogenic heat flux into the atmosphere. The ventilation rate within the urban canopy layer is followed Yang et al. [5]. Note here that the rural air temperature can be

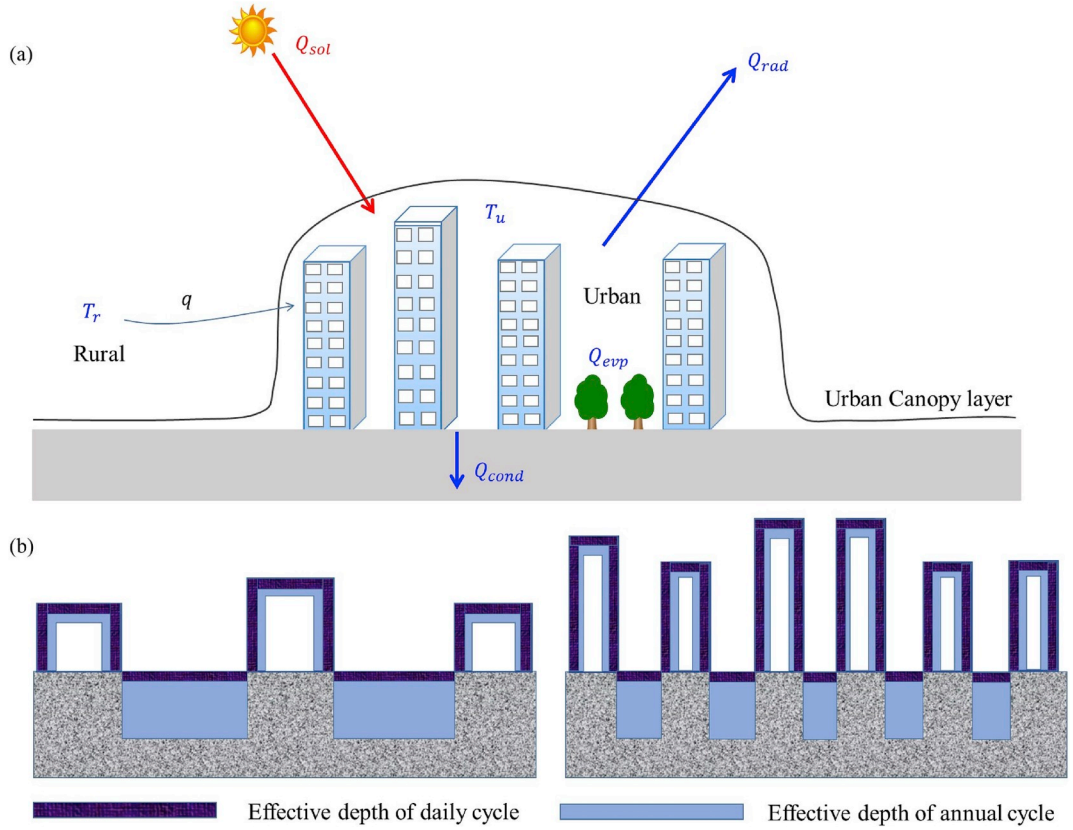

Fig. 1. (a) Schematic illustration of the lumped urban air temperature model in an idealized urban area. (b) An illustration of the differences between the effective depth for the daily and annual cycles on different building configurations.

approximated written by using Fourier series $T_r = \overline{T_r} + \sum_{j=1}^{n}(T_{r1j}\cos j\omega t + T_{r2j}\sin j\omega t)$[22].

The energy balance equation in the model provided by Yang et al. [5] is written as

$$mC_s\frac{dT_s}{dt} = (1-\alpha)Q_{sol}A_p\downarrow - Q_{evp}A_{pn}\uparrow - Q_{conv}A_b\uparrow - Q_{cond}A_b\uparrow - Q_{rad}A_b\uparrow \tag{4}$$

Downward and upward errors denote downwelling and upwelling processes. mC_s is the thermal mass of the urban surfaces. For simplicity, Q_{evp} can be described as $Q_{evp} = E_t\rho_{H_2O}L_v$, Q_{conv} can be described as $Q_{conv} = h_c(T_s - T_u)$. Q_{rad} can be written as $Q_{rad} = h_{rad}(T_s - T_{sky})$, where the long-wave radiation coefficient is simplified as $h_{rad} = 4\varepsilon\sigma\overline{T}^3$. T_{sky} is the effective sky temperature. $\overline{T}$ is the mean of T_s and T_{sky}. For more details on Equation (4), please refer to Refs. [5,19].

In this model, the conductive heat transfer, Q_{cond}, can be written as

$$Q_{cond} = \lambda_p\frac{T_s - T_m}{\Delta z} \tag{5}$$

where T_m is the sub-surface temperature of the urban surfaces; Δz is the penetration depth of the urban surfaces where the daily temperature variation can be ignored.

2.2. Improved lumped urban air temperature model

The improved model contains both the city air energy balance and the city surface energy balance. The city air energy balance is the same as Yang et al. [5]. While the city surface energy balance is:

$$Q_{cond(0,t)}A_b = (1-\alpha)Q_{sol}A_p\downarrow - Q_{evp}A_{pn}\uparrow - Q_{conv}A_b\uparrow - Q_{rad}A_b\uparrow \tag{6}$$

The urban surfaces are assumed to be homogeneous. The one-dimensional heat conduction through urban surfaces becomes [23,24]:

$$\frac{\partial T_s}{\partial t} = \frac{\lambda_p}{\rho_s C_s}\frac{\partial^2 T_s}{\partial z^2} \tag{7}$$

Note here that the unknown diurnal variation of urban surface temperature, T_s, can be approximated using Fourier analysis [23,24]:

$$T_s(0,t) = \overline{T_s} + \sum_{j=1}^{n}\left(T_{s1j}\cos j\omega t + T_{s2j}\sin j\omega t\right) \tag{8}$$

where j means different harmonics and ω is the frequency. The solution of Equation (5) becomes [23,24]:

$$T_s(z,t) = \overline{T_s} + \sum_{j=1}^{n} e^{-\frac{z}{d_j}}\left[T_{s1j}\cos\left(j\omega t - \frac{z}{d_j}\right) + T_{s2j}\sin\left(j\omega t - \frac{z}{d_j}\right)\right] \tag{9}$$

where $d_j = \sqrt{\frac{2\lambda_p}{j\omega\rho_s C_s}}$ is the penetration depth of the force and the higher harmonics have a small penetration depth. The $Q_{cond(0,t)}$ of Equation (4) can be rewritten as:

$$Q_{cond(0,t)} = -\lambda_p\frac{dT_s(z,t)}{dz}\bigg|_{z=0} = \lambda_p\sum_{j=1}^{n}\frac{1}{d_j}\left[\left(T_{s1j}+T_{s2j}\right)\cos j\omega t + \left(T_{s2j}-T_{s1j}\right)\sin j\omega t\right] \tag{10}$$

2.3. Estimating change in daily and annual thermal mass in urban areas

The substitution of natural surfaces with artificial materials such as roofs, walls, and streets, allows more heat to be stored in the thermal mass and slowly released during the night time [25]. The depth of these surfaces capable of storing heat is effectively the same as that capable of sensing surrounding temperature change, which can thus be calculated

in terms of effective depth. The effective depth, d_{ej}, of a temperature cycle can be calculated as $\sqrt{\frac{\lambda_p}{2j\omega\rho_s C_s}}$ [26,27]. The effective depth using in the force-restore method is the ground depth at which the temperature is assumed to be the same as the surface temperature to consider the thermal-storage effect [26]. This study uses this method to estimate the thermal mass in the urban areas. Effective depth differs significantly between daily and annual cycles, which $j\omega$ is different, as shown in Fig. 1b. If the average thermal diffusivity, a_p, of soil and concrete is approximately 0.5 mm^2 s^{-1}, the effective depth for daily and annual cycles is 0.06 m and 1.12 m, respectively. The effective depth of annual cycle is 18.6 times greater than the daily cycle. For reference, Table S1 summarizes the effective-depth values calculated for different construction materials and ground materials, assuming that these materials constitute a semi-infinite homogeneous medium. Manmade structures such as building envelopes and street pavement (concrete, asphalt) are typically less than 0.1–0.2 m thick or deep [28,29]. As the daily effective depth is close to 0.1 m, most of the thermal-storage potential of a manmade structure can be utilized by a daily temperature cycle. Fig. 1b shows the daily and annual thermal mass in the different city morphology. In the high rose and high compact city like Hong Kong, the total area of the exterior surfaces of vertical walls and roofs is roughly five times greater than the land area [5]. The buildings in such a city act like fins in a heat exchanger. The building surfaces effectively increase the heat transfer surface area of a given area of covered land. An increased heat transfer area increases the thermal storage available for the daily cycle.

2.4. Analytical solution of improved lumped urban air temperature model

The solution contains three parts, the mean urban air temperature; and the amplitude and phase term, respectively. First, three parameters are defined: the relative convective heat transfer number, $\lambda = \frac{h_c A_b}{\rho C_p q}$; relative sky radiation heat transfer number, $\lambda_{sky} = \frac{h_{rad} A_b}{\rho C_p q}$; and time constant, $\tau_j = \frac{d_{ej}\rho_s C_s A_b}{\rho C_p q}$.

An effective urban heat flux Q is then defined as follows:

$$Q = (1-\alpha)A_p Q_{sol} - A_{pn} Q_{evp} + \left(1 + \frac{\lambda_{sky}}{\lambda}\right) A_p Q_{anth} \tag{11}$$

The mean urban air temperature $\overline{T}_u$, and the second and third are the amplitude, ΔT_{uj}, and phase, Φ_{uj} are as follows

$$\overline{T}_u = \frac{\lambda + \lambda_{sky}}{\lambda + \lambda_{sky} + \lambda\lambda_{sky}} \overline{T}_r + \frac{\lambda}{\lambda + \lambda_{sky} + \lambda\lambda_{sky}} \lambda_{sky} \overline{T}_{sky} + \frac{1}{\lambda + \lambda_{sky} + \lambda\lambda_{sky}} \lambda \overline{T}_Q \tag{12}$$

$$\Delta T_{uj} = \frac{\sqrt{f_1 \Delta T_{rj}^2 + f_2 \Delta T_{Qj}^2 + 2 f_1 f_2 \Delta T_{rj} \Delta T_{Qj} \cos\left(\varphi_{rj} + \Delta\Phi_{rj} - \Phi_{Qj} - \Delta\Phi_{Qj}\right)}}{(1+\lambda)^2 \left[\gamma^2 + (j\omega\tau_j)^2\right]} \tag{13}$$

$$\tan\Phi_{uj} = \frac{\left(\tan\Phi_{rj} + \tan\Delta\Phi_{rj}\right) + \tan\Phi_{rQ}\frac{\Delta T_{Qj}}{\Delta T_{rj}}\left(\tan\Phi_{Qj} + \tan\Delta\Phi_{Qj}\right)}{\left(1 - \tan\Phi_{rj}\tan\Delta\Phi_{rj}\right) + \tan\Phi_{rQ}\frac{\Delta T_{Qj}}{\Delta T_{rj}}\left(1 - \tan\Phi_{Qj}\tan\Delta\Phi_{Qj}\right)} \tag{14}$$

where $\gamma = (j\omega\tau_j) + \frac{\lambda}{1+\lambda} + \lambda_{sky}$, $f_1 = [(1+\lambda)(\gamma^2 + (j\omega\tau_j)^2) + \lambda^2\gamma]^2 + (\lambda^2(j\omega\tau_j))^2$, $f_2 = (\lambda\gamma)^2 + (\lambda j\omega\tau_j)^2$, $\tan\Phi_{rj} = \frac{T_{r2j}}{T_{r1j}}$, $\tan\Delta\Phi_{rj} = \frac{\lambda^2(j\omega\tau_j)}{(1+\lambda)[\gamma^2+(j\omega\tau_j)^2]+\lambda^2\gamma}$, $\tan\Phi_{Qj} = \frac{T_{Q2j}}{T_{Q1j}}$, and $\tan\Delta\Phi_{Qj} = \frac{j\omega\tau_j}{\gamma}$. $\Delta T_{rQ} = 2\sqrt{f_1 f_2}\Delta T_{rj}\Delta T_{Qj}\cos(\Phi_{rj} + \Delta\Phi_{rj} - \Phi_{Qj} - \Delta\Phi_{Qj})$, which stands for the interaction between the rural air temperature and the temperature rise T_Q due to the effective urban heat flux, Q. ΔT_{rj} and ΔT_{Qj} represent the amplitude of rural air temperature and effective urban heat flux Q, respectively.

2.5. The relationship between two lumped air temperature models

As mentioned above, both the lumped air temperature models has two energy balance, which are the city air energy balance and urban surface energy balance. For the two models, there are two methods for the urban surface energy balance, which can be found in Equations (3) and (4 and 6), respectively. The T_m and Δz in Equation (5) in the previous model is chosen based on empirical or model studies [5]. From the improved model, following the FFT expansion of surface temperature in Equation (8), and combine Equations (6), (8) and (9), then obtain:

$$\lambda_p \sum_{j=1}^{n} \alpha_j \left[(T_{s1j} + T_{s2j})\cos j\omega t + (T_{s2j} - T_{s1j})\sin j\omega t\right] = (1-\alpha)Q_{sol}A_p\downarrow - Q_{evp}A_{pn}\uparrow - Q_{conv}A_b\uparrow - Q_{rad}A_b\uparrow \tag{15}$$

Then the mean urban surface temperature can be obtained from Equations (3) and (15):

$$(1+\lambda)\left[(1-\alpha)Q_{sol}A_p - Q_{evp}A_{pn}\right] + \lambda Q_{anth}A_p + (1+\lambda)h_{rad}A_b\overline{T_{sky}} + h_c A_b \overline{T_r} - [h_c + h_{rad}(1+\lambda)]A_b\overline{T_s} = 0 \tag{16}$$

For the previous lumped model, following the FFT expansion of surface temperature in Equation (8), and combine Equations (4) and (5), then obtain:

$$mC_s \sum_{j=1}^{n} j\omega\left[T_{s2j}\cos(j\omega t) - T_{s1j}\sin(j\omega t)\right] = (1-\alpha)Q_{sol}A_p\downarrow - Q_{evp}A_{pn}\uparrow - Q_{conv}A_b\uparrow - Q_{cond}A_b\uparrow - Q_{rad}A_b\uparrow \tag{17}$$

Then the mean urban surface temperature can be obtained from Equations (3) and (17):

$$(1+\lambda)\left[(1-\alpha)Q_{sol}A_p - Q_{evp}A_{pn}\right] + \lambda Q_{anth}A_p + (1+\lambda)h_{rad}A_b\overline{T_{sky}} + h_c A_b\overline{T_r} + \lambda_p A_b\frac{(1+\lambda)}{\Delta z}T_m - \left[h_c + h_{rad}(1+\lambda) + \lambda_p\frac{(1+\lambda)}{\Delta z}\right]A_b\overline{T_s} = 0 \tag{18}$$

Then T_m can be determined, and $T_m = \overline{T_s}$.

In Section 2.4, three non-dimensional numbers are introduced to solve the two energy balances and to present physical meaning of urban air temperature. One of the three parameters is time constant number, which is defined as $\tau_j = \frac{d_{ej}\rho C_p A_b}{\rho C_p q}$. For the previous model introduced by Yang et al. [5], there is a new term, which is the conductive heat transfer term, $\lambda_p\frac{T_s - T_m}{\Delta z}$. To solve the two energy balance, a new relative conduction heat transfer number needs to be introduced, which is $\lambda_k = \frac{\lambda_p\frac{A_b}{\Delta z}}{\rho C_p q}$. From the point of physical meaning, the time constant number, τ_j and relative conduction heat transfer number, λ_k has the same meaning, which considers the heat transfer into the sub-surfaces through heat conduction. Then Δz, which is the penetration depth of the urban surfaces where the daily temperature variation can be ignored, can be obtained: $\Delta z = 2d_{ej}$.

3. Results and discussion

3.1. Model evaluation with the observation data in the city of Hong Kong

In this section, Kowloon Peninsula, Hong Kong (22°15′N, 114°15′E) is chosen as the target area with a plan area of 47 km^2. With a total population of 7.2 million (Census and Statistics Department, HKSAR) in a total area of 1095 km^2, the urban area occupying merely 20% of the land is one of the most dense areas in the world. The urban area of Hong Kong is a high-dense and high compact area with tremendous number of high buildings, typically 20–40 floors. Two weather stations (Fig. 2), Hong Kong Observatory Headquarters (HKO, 32 m, 22°18′07″N, 114°10′27″E, located in Tim Sha Tsui, the core urban area of Kowloon) and Ta Kwu Ling (TKL, 15 m, 22°31′43″N, 114°09′24″E, located in the

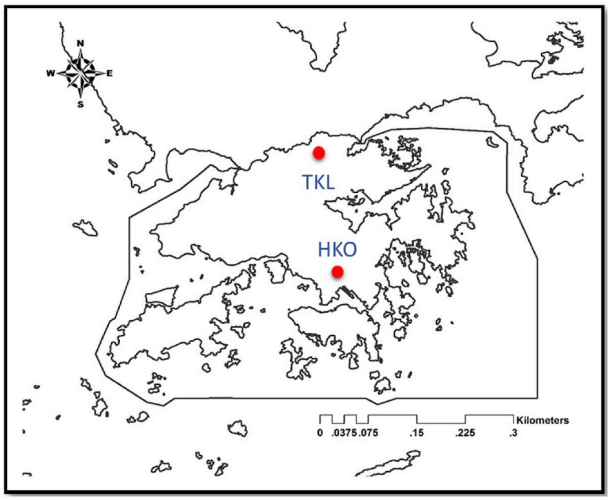

Fig. 2. Hong Kong map with the locations of urban site (HKO) and rural site (TKL).

northeast of the New Territories with lush vegetation but low dense population) are chosen as urban and rural area, respectively. The distance between TKL and HKO is around 25 km. To better understand the daily cycle of urban air temperature, the calm and cloudless days are chosen for analysis from 1994 to 2013 based on the following criteria: precipitation days and the day after the precipitation days are excluded; wind speed $\leq$5 m/s and cloud amount $\leq$2 oktas during the day. The meteorological data containing daily mean air temperature in TKL, wind speed, cloud amount, solar radiation, evapotranspiration, relative humidity, rainfall amount are provided as input data in the model. In this section, the measurement equipment will not be illustrated, and the details can be found at www.weather.gov.hk.

Lists of input parameters for urban morphology and surface material thermal properties are provided in Table 1. Values of the urban morphology data in Kowloon Peninsula are based on analysis of GIS data. The values of the thermal properties in Table 1, which are fixed in this chapter, are adopted and selected from the literature [5,17,22,30–32]. Δz and T_m are chosen from Yang et al. [5]. Fig. 3a shows results of the prediction of urban air temperature from two lumped models and the observation data from urban and rural sites in July from Year 1994–2013. The model can reasonably recapture the basic characteristics of the urban air temperature, both in the phase and amplitude. Due to the uncertainty of the two variables in Yang's model, the model overestimates the thermal storage in the urban areas. Hence the previous model can not well capture the time and value of maximum air temperature. Δz and T_m are two important variables that could influence the urban thermal mass especially in the high rise and high compact city. The improved model shows the maximum temperature occurring at the time 3:42 p.m. with the value of 32.35 °C and is half an hour delayed and 0.15 °C lower in compared to the measurement data. The minimum temperature is 27.16 °C occurring at 6:20 a.m., which is 0.64 °C lower than the measured data at HKO. The maximum and minimum temperature of the improved model are in agreement with the observed data though slightly offset in time. The diurnal temperature range are 5.18 °C and 4.72 °C for the improved model and measured data, respectively. The statics method [33] including coefficient of determination (R^2), root-mean-square error (RMSE) and mean bias error (MBE), has been used to evaluate the model performance. The improved model presents reasonable agreement with R^2 larger than 0.96 and RMSE less than 0.37 °C.

3.2. Impacts of building configurations in the urban areas

In this section, the impact of building configurations on the daily cycle of urban air temperature is investigated. Two experiments are carried out. The first (a) is to change the building height but maintain the plan area per unit ground area ($f_s + f_r$) as constant, which influence f_w and also ventilation rate. The second (b) is to change plan area per unit ground area but the mean building height, h as constant, which influence the relationship between f_r, f_s and f_n, as shown in Fig. 4 and Table 2.

The comparison (a) focuses on the impact of building height on the three components of the urban air temperature. Fig. 5 presents the trend of the mean value, amplitude and phase shift of the urban air temperature based on the variation of building height. The plan area per unit ground area is 0.55. The results show that the mean air temperature and amplitude sharply decrease initially and then it tends to stabilize if continuously increasing the building height. Increase of the building height will increase the built area of the urban areas, and the relative convective heat transfer number, λ, will increase. Furthermore, the urban surface temperature has a more powerful impact on the urban air temperature. When the building height increases to satisfy the high compact and high dense city criteria, the solar radiation may not go through the urban street due to the shadow areas and block effect in the area [2,5,6]. In the high rise and high compact scenario, there exists more urban surfaces for thermal storage due to the larger building wall areas. In real situation, the sky view factor also declines when increasing the building height [6]. When the building height is lower, both the

Table 1
Input urban morphology and thermal properties parameters.

	Variable	Symbol	Input parameters	Source
Urban morphology input data	Urban plan area (km^2)	A_p	47	Estimated based on GIS data [5],
	Total built area (km^2)	A_b	305.5	Estimated based on GIS data [5,30,31],
	Fraction of pavement roads on plan area (−)	f_s	0.25	[5,30,31]
	Fraction of building roofs on plan area (packing density) (−)	f_r	0.55	[5,17]
	Fraction of natural surfaces on plan area (−)	f_n	0.20	[5,17,22]
	Fraction of building walls on plan area (−)	f_w	5.5	[5,17,22]
	Urban area control volume height (m)	h	55.2	Estimated based on GIS data
	Latitude (north positive) (rad)	ϕ	22.25	Google earth
	Longitude (east positive) (rad)	ψ	114.25	Google earth
Urban thermal properties input data	Urban albedo (−)	α	0.30	[5,17]
	Emissivity of urban areas (−)	ε	0.90	[5,17]
	Thermal conductivity of urban areas (W K^{-1} m^{-1})	λ_p	1.0	[5,17]
	Volumetric heat capacity of urban surfaces (MJ K^{-1} m^{-3})	$\rho_s C_s$	2.40	[5,17]
	Mean evaporation rate (W/m^2)	$\overline{Q_{evp}}$	90	Measured data
	Mean anthropogenic heat (W/m^2)	$\overline{Q_{anth}}$	20	Estimated based on [32]

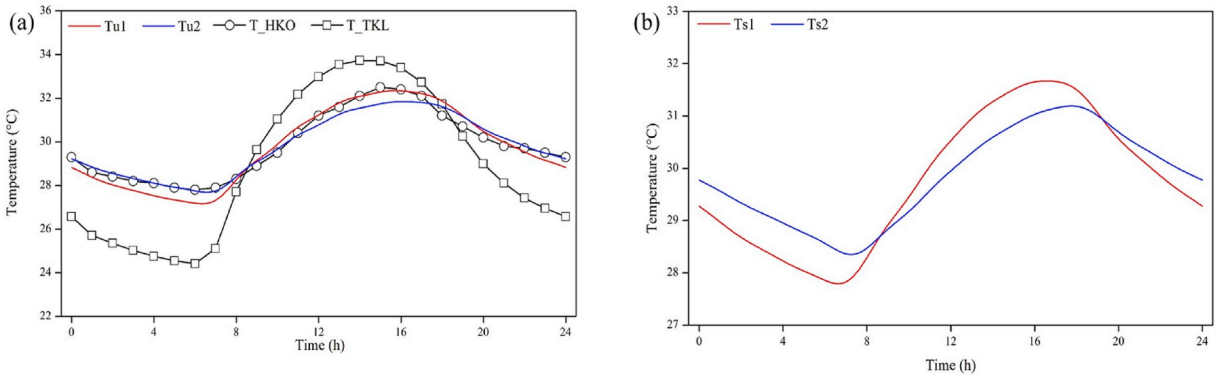

Fig. 3. (a) Predicted daily cycle of urban air temperature from the improved and previous lumped air temperature model and observed urban and rural 2 m air temperature at HKO and TKL station in July from Year 1994–2013. (b) Predicted daily cycle of urban surface temperature from the improved and previous lumped air temperature model. T_{u1} and T_{s1} stand for the improved model.

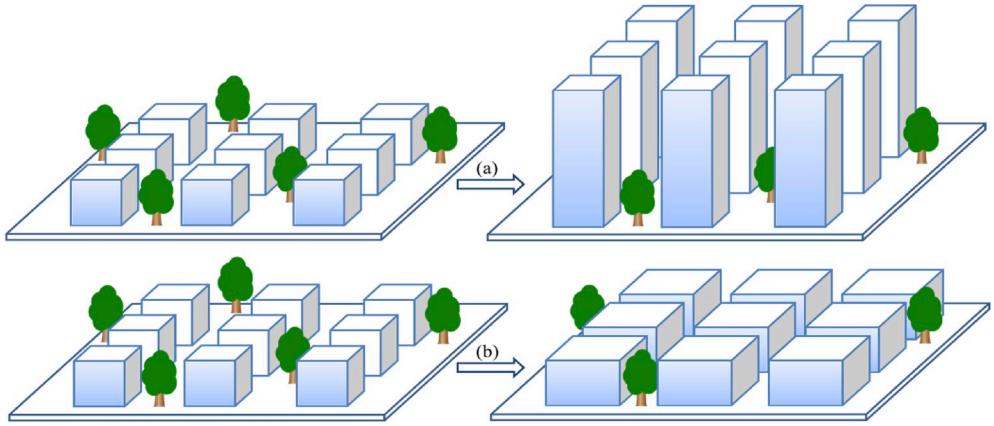

Fig. 4. Schematic illustration of two experiments.

Table 2
Urban canopy geometry in the two experiments.

Scenario No.	(a) h (m)	(b) f_n
1	10	0
2	20	0.1
3	30	0.2
4	40	0.3
5	50	0.4
6	60	0.5
7	70	0.6
8	80	0.7
9	90	–
10	100	–

absorbed solar radiation and long wave radiation is larger, which contributes the high surface temperature. The solar radiation dominates the surface temperature within the urban canopy and further influence the air temperature. Therefore, the thermal environment for the high rise and high compact city may be better than the low rise city during the day. It is possible for the cool island phenomenon to appear, but the circumstance is opposite during the night as more thermal storage should be emitted.

The second experiment (b) is carried out under different natural surfaces ratio. Note that the urban albedo, sky view factor and ventilation rate are unchanged in this case. However, the wind velocity may decrease in the high compact and high dense city [6,8,13]. As the natural surfaces increase, with respect to the decrease of building density, the mean temperature value slightly increases; the phase shift advances while the amplitude increases (as shown in Fig. 6). When building density decreases, which means that the thermal storage is lower, then the phase shift is advanced and combined with the large diurnal temperature range. Due to the decrease of the built area by increasing the natural surfaces within the urban canopy layer, the relative convection heat transfer number, λ, decreases, which implies that the convective heat transfer between the urban surfaces and ambient air reduces. If the other factors being unchanged, the mean air temperature value will increase due to larger absorbed solar radiation because of less blockage for the solar radiation to get through and less urban surfaces for thermal storage. The evaporation/evapotranspiration is enhanced due to the large area of the natural surfaces, the ambient air temperature around the natural surfaces area may experience lower than the other areas [34].

3.3. Impacts of anthropogenic heat

Anthropogenic heat is the heat released into the atmosphere due to human activities which include transportation, industrial, residential and commercial buildings, human activities [25], which varies both diurnally and seasonally [32]. The anthropogenic heat and air pollution are generally removed by the wind, but in the high rise and high compact city like Hong Kong, the buildings may influence the approaching wind with the large and strong drag effect [35]. So the air pollution and anthropogenic heat may not be removed timely. Fig. 7 provides the diurnal profile of urban air temperature under different anthropogenic heat release into the atmospheric environment. The

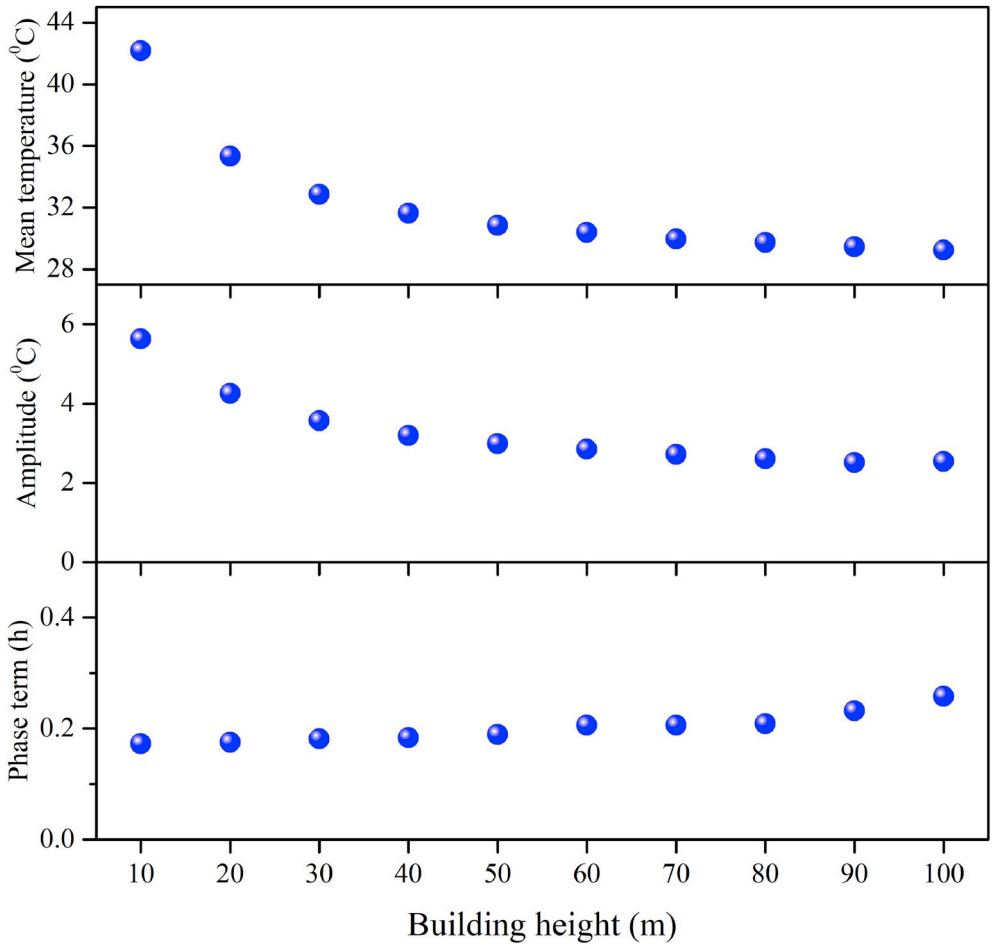

Fig. 5. Urban air temperature in terms of mean temperature, amplitude and phase term for different f_n ratio.

relative temperature rise due to anthropogenic heat $T_E = \frac{A_p Q_{anth}}{\rho C_p q}$ is influenced by ventilation rate in the urban areas. If the anthropogenic heat strength is double and maintain the ventilation rate unchanged, thus will cause increase of T_E and urban air temperature (shown in Fig. 7). The mean, maximum and minimum value increase when increasing the anthropogenic heat release. The different anthropogenic heat release scenarios has less impact on the amplitude phase term. Yang et al. [5] has shown that the turbulence air change is lower in the high rise and high compact city which will influence the air change rate within the urban canopy layer. Thus will further influence the heat and pollutant removal from the urban areas. However, the urban cool island phenomenon easily disappear as the anthropogenic heat releases, as illustrated by Yang et al. [5].

3.4. Discussions

As mentioned above, the factors, which includes building configurations and anthropogenic heat, have significant effects on the three components of urban air temperature. From the solution of the lumped urban air temperature model, the urban air temperature is the modification of the rural air temperature with other combined factors. In this section, the mean temperature, amplitude and phase term of urban air temperature in comparison to the corresponding rural air temperature is conducted.

The mean urban air temperature is a weighted average of the rural air temperature $\overline{T}_r$, the effective temperature of the sky $\overline{T}_{sky}$, and the temperature rise $\overline{T}_Q$ due to the effective urban heat flux, Q, and is also determined by the relative convective heat transfer number, λ, and relative sky radiation heat transfer number, λ_{sky}, and is not determined by the time constant number, τ_j (shown in Equation (13)). When the relative convective heat transfer number, $\lambda = 0$, which means that the convective heat transfer at the urban surfaces is absent [22], the mean urban air temperature is rewritten as follows:

$$\overline{T_u} = \overline{T_r} + \overline{T_E} \quad (19)$$

At this time, the mean urban air temperature is simply the modification of mean rural air temperature by temperature rise due to anthropogenic heat. If the anthropogenic heat tends to zero within the urban canopy layer, then the urban mean air temperature is equal to the rural mean air temperature, $\overline{T_u} = \overline{T_r}$. The urban mean air temperature is always higher than the rural mean air temperature.

The first harmonic (j = 1) of the urban air temperature and rural air temperature describes fairly well the total amplitude and time for maximum temperature whereas the time for the minimum temperature is highly influenced by the other harmonics [23,24]. Fig. 8 provides the first and second harmonic of the rural air temperature. In this case, only the first harmonic of the rural air temperature is considered. Note that the variation of the combined heat is ignored here.

Similar to other studies [22], the rural air temperature can be expressed as:

$$T_r = \overline{T_r} + \Delta T_{r1} \cos(\omega t) \quad (20)$$

The two coefficients of the first harmonic (j = 1) of the urban air temperature are T_{u11} and T_{u21}, or simply written as

$$T_u = \overline{T_u} + T_{u11} \cos \omega t + T_{u21} \sin \omega t = \overline{T_u} + \Delta T_{u1} \cos(\omega t + \phi_0) \quad (21)$$

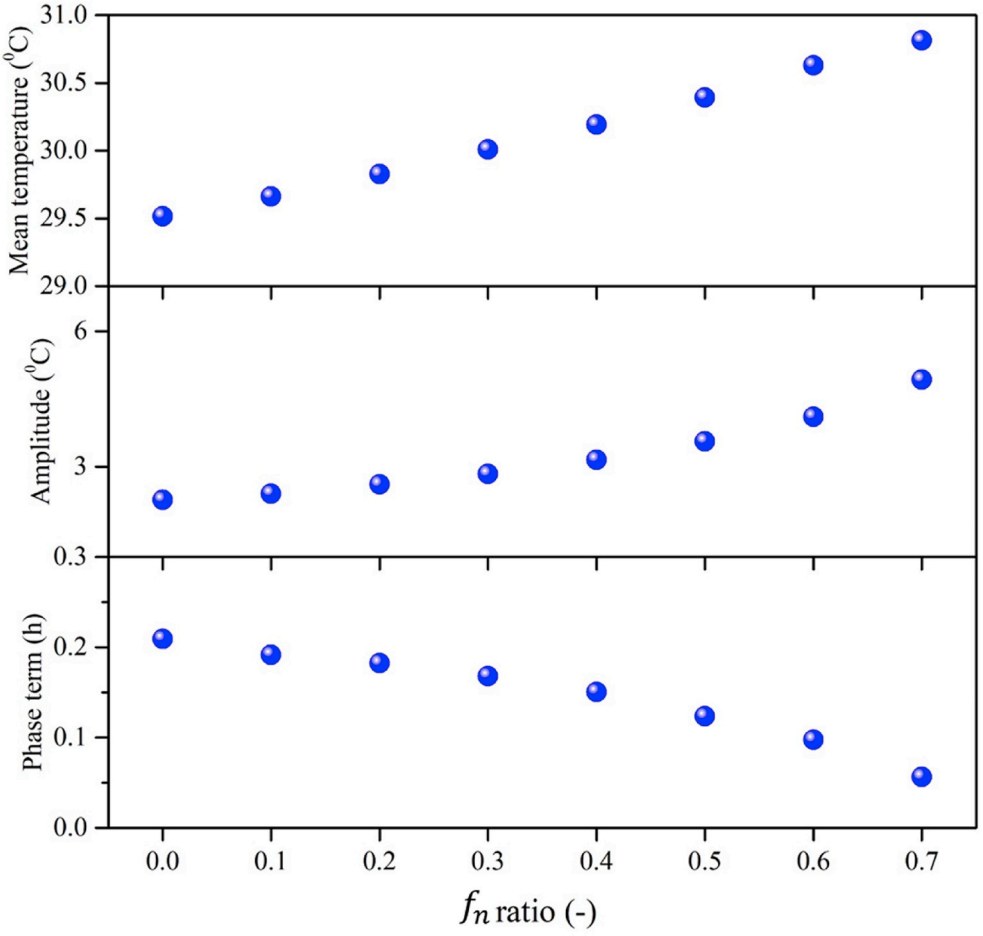

Fig. 6. Urban air temperature in terms of mean temperature, amplitude and phase term for different building height level.

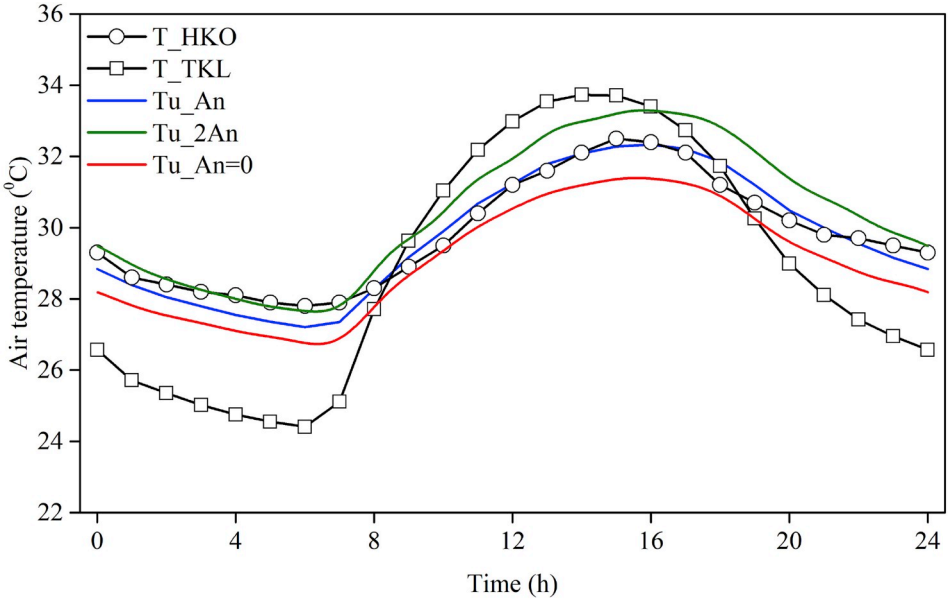

Fig. 7. Daily cycle of urban air temperature under different anthropogenic heat strength.

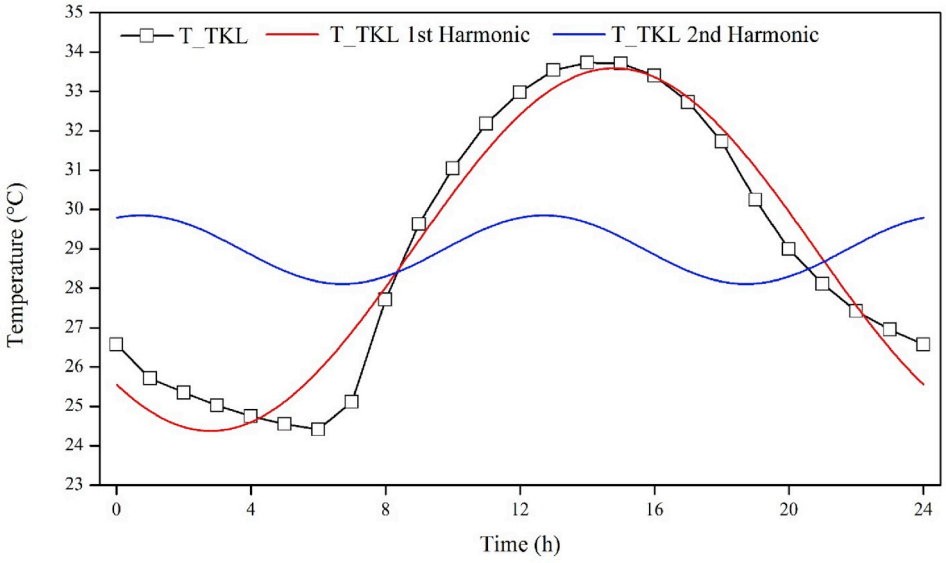

Fig. 8. 1st and 2nd harmonic of Fourier expansion of the rural air temperature.

where

$$\Delta T_{u1} = \sqrt{T_{u11}^2 + T_{u21}^2}\cos(\omega t + \phi_0) \tag{22}$$

$$\phi_0 = -\arctan\left(\frac{T_{u21}}{T_{u11}}\right) \tag{23}$$

Then the amplitude ratio and phase shift of urban and rural air temperature is obtained, as shown in Table 3.

Fig. 9 provides the amplitude ratio and phase shift of urban air temperature with respect to the rural air temperature as a function of relative convective heat transfer and time constant number. It can be shown from Fig. 9 that increasing the time constant number, τ, leads to the initial decrease of the amplitude ratio and then achieve the stabilization value, and increasing the relative convective heat transfer number, λ, leads to fast declination of amplitude ratio. When the relative heat transfer number tends to zero, which means that the ventilation effect is more significant under this circumstances. Hence, the amplitude of the urban air temperature is almost equilibrium with the incoming rural air temperature. When the relative convective heat transfer number enlarges, which means that the relative effect of convection heat transfer between the urban surfaces and the urban air is more significant than the ventilation effect, the amplitude ratio is decreased. This means that the less ventilation rate which can bring the rural air into the city and dilute the air pollution. With the larger value of λ, the small variation of the urban air temperature is obtained but people suffering the low ventilation rate within the urban canopy layer.

The phase shift is shown in Fig. 9. If λ tends to zero, which means that the convective heat transfer is absent, the phase shift is zero. Thus illustrates that when ventilation effect is infinite, the phase shift of the urban air temperature with respect to the rural air temperature is almost zero. There is no phase delayed in such situation. With the increase of λ, the phase is delayed. As the time constant increases, the phase delayed phenomenon increases. When the relative convective heat transfer number is larger and tends to infinite, the heat transfer resistance between the urban surfaces and urban air is absent and the advection heat transfer becomes negligible, which leads to the urban surface temperature in equilibrium with the urban air temperature. So when continuously increasing the urban fabric volume, which directly increasing the demand storage heat in the urban surfaces, it leads to the slow increasing rate of the urban surface temperature and then indirectly influences the grow rate of the urban air temperature.

Table 3
Amplitude ratio and phase shift of urban and rural air temperature.

Amplitude ratio (−), $\frac{\Delta T_{u1}}{\Delta T_{r1}}$	Phase shift (h), ϕ_0
$\sqrt{\frac{\lambda^2 + 2\lambda\omega\tau + 2(\omega\tau)^2}{((1+\lambda)\omega\tau)^2 + (\lambda + (1+\lambda)\omega\tau)^2}}$	$-\arctan\left(\frac{\lambda^2\omega\tau}{\lambda^2(1+\omega\tau) + 2\omega\tau[\lambda + (1+\lambda)\omega\tau]}\right)$

4. Conclusions

An improved lumped urban air temperature model is provided, which aims not to accurately predict the urban air temperature cycle, but to understand the physical mechanisms of the diurnal cycle of urban air temperature and to provide quantitative understanding of impact of building configurations and anthropogenic heat on urban thermal environment. The diurnal urban air temperature is characterized by mean temperature, amplitude and phase term. The method to estimate the thermal mass in the urban areas is introduced. The improved method can obtain two variables in the previous model, the sub-surface temperature of the urban surfaces, T_m, and the penetration depth of the urban surfaces where the daily temperature variation can be ignored, Δz. These two variables play an important role in the urban thermal mass especially in the high rise and high compact city, but are usually determined based on other model studies.

The model is compared with averaged summer observation data from Hong Kong over a period of 19 years. The improved model can reasonably recapture the basic characteristics of the urban air temperature, both in the phase and amplitude. Due to the uncertainty of the two variables in Yang's model, the model overestimates the thermal storage in the urban areas. Hence the previous model can not well capture the time and value of maximum air temperature.

The improved model is then used to analyze the impact of building configurations and anthropogenic heat on urban thermal environment. When increase the building height, the urban thermal storage increase but the solar radiation penetrating into the urban canopy layer deceases. Therefore, the thermal environment for the high rise and high compact city may be better than the low rise city during the day. It is possible for the cool island phenomenon to appear, but the circumstance is opposite during the night as more thermal storage should be emitted. When the natural surfaces increase, with respect to the decrease of building density, the mean temperature value slightly increases; the phase shift advances while the amplitude increases. The mean, maximum and

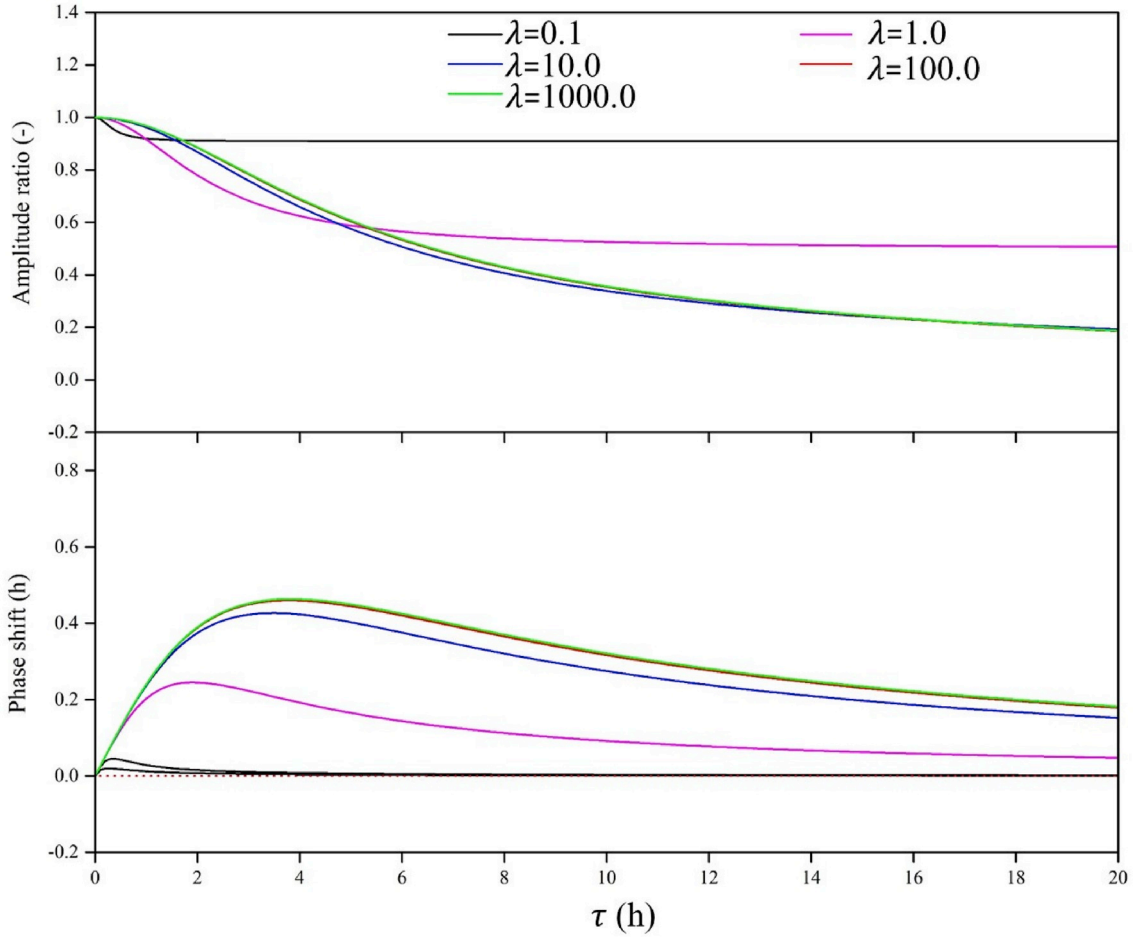

Fig. 9. Amplitude ratio and phase shift as a function of time constant τ, and relative convective heat transfer number, λ.

minimum value increase when increasing the anthropogenic heat release. The different anthropogenic heat release scenarios has less impact on the amplitude phase term. However, the urban cool island phenomenon disappears easily if increase the anthropogenic heat.

Two important parameters for engineers are emphasized, relative convective heat transfer number, λ, and time constant, τ. Under the fixed relative convective heat transfer number, λ, increasing the time constant number, τ, leads to the initial decrease of the amplitude ratio and significant phase delay. Increasing the relative convective heat transfer number, λ, leads to fast declination of amplitude ratio and the phase delayed. When the relative heat transfer number tends to zero, which means that the ventilation effect is more significant under this circumstances, both the amplitude and phase of the urban air temperature is almost equilibrium with the incoming rural air temperature. These two parameters could provide engineers and urban planners principles on the urban design. The two parameters also provide some insights on how to control the urban thermal environment in an engineering way.

Declaration of competing interests

The authors declare that they have no known competing financial interests or personal relationships that could have appeared to influence the work reported in this paper.

Acknowledgements

Yu Xue is supported by the National Natural Science Foundation of China (Grant No. 51708084). The National Center for Atmospheric Research (NCAR) is sponsored by the National Science Foundation (NSF). Yi Wang thanks the NCAR Advanced Study Program (ASP) Fellowship sponsored by NSF. Jin Shen is supported by the Guangdong special fund for science and technology development (2017B020216007). The weather data for individual stations were obtained through collaboration with Hong Kong Observatory. The input and output data used in this study are available upon request from corresponding author, which are used for academic research purpose.

Appendix ASupplementary data

Supplementary data to this article can be found online at https://doi.org/10.1016/j.buildenv.2019.106564.

References

[1] R. DeFries, Terrestrial vegetation in the coupled human-earth system: contributions of remote sensing, Annu. Rev. Environ. Resour. 33 (2008) 369–390.
[2] T.R. Oke, The distinction between canopy and boundary-layer urban heat islands, Atmosphere 14 (4) (1976) 268–277.
[3] E. Kalnay, M. Cai, Impact of urbanization and land-use change on climate, Nature 423 (6939) (2003) 528–531.
[4] W. Zhan, W. Ju, S. Hai, G. Ferguson, J. Quan, C. Tang, F. Kong, Satellite-derived subsurface urban heat island, Environ. Sci. Technol. 48 (20) (2014) 12134–12140.
[5] X. Yang, Y. Li, Z. Luo, P.W. Chan, The urban cool island phenomenon in a high-rise high-density city and its mechanisms, Int. J. Climatol. 37 (2) (2017) 890–904.
[6] X. Yang, Y. Li, Development of a three-dimensional urban energy model for predicting and understanding surface temperature distribution, Boundary-Layer Meteorol. 149 (2) (2013) 303–321.
[7] Z. Bottyán, J. Unger, A multiple linear statistical model for estimating the mean maximum urban heat island, Theor. Appl. Climatol. 75 (3) (2003) 233–243.
[8] J. Hang, Y. Li, Macroscopic simulations of turbulent flows through high-rise building arrays using a porous turbulence model, Build. Environ. 49 (2012) 41–54.

[9] A. Kantzioura, P. Kosmopoulos, S. Zoras, Urban surface temperature and microclimate measurements in Thessaloniki, Energy Build. 44 (2012) 63–72.
[10] M. Lin, J. Hang, Y. Li, Z. Luo, M. Sandberg, Quantitative ventilation assessments of idealized urban canopy layers with various urban layouts and the same building packing density, Build. Environ. 79 (2014) 152–167.
[11] X. Yang, Y. Li, The impact of building density and building height heterogeneity on average urban albedo and street surface temperature, Build. Environ. 90 (2015) 146–156.
[12] G. Guo, X. Zhou, Z. Wu, R. Xiao, Y. Chen, Characterizing the impact of urban morphology heterogeneity on land surface temperature in Guangzhou, China, Environ. Model. Softw 84 (2016) 427–439.
[13] Y. Wang, S. Di Sabatino, A. Martilli, Y. Li, M.S. Wong, E. Gutiérrez, P.W. Chan, Impact of land surface heterogeneity on urban heat island circulation and sea-land breeze circulation in Hong Kong, J. Geophys. Res.: Atmosphere 122 (8) (2017) 4332–4352.
[14] J. Kondo, T. Watanabe, Studies on the bulk transfer coefficients over a vegetated surface with a multilayer energy budget model, J. Atmos. Sci. 49 (23) (1992) 2183–2199.
[15] A. Martilli, A. Clappier, M.W. Rotach, An urban surface exchange parameterisation for mesoscale models, Boundary-Layer Meteorol. 104 (2) (2002) 261–304.
[16] H. Kondo, Y. Genchi, Y. Kikegawa, Y. Ohashi, H. Yoshikado, H. Komiyama, Development of a multi-layer urban canopy model for the analysis of energy consumption in a big city: structure of the urban canopy model and its basic performance, Boundary-Layer Meteorol. 116 (3) (2005) 395–421.
[17] Z.H. Wang, E. Bou-Zeid, J.A. Smith, A coupled energy transport and hydrological model for urban canopies evaluated using a wireless sensor network, Q. J. R. Meteorol. Soc. 139 (675) (2013) 1643–1657.
[18] F. Chen, H. Kusaka, R. Bornstein, J. Ching, C.S.B. Grimmond, S. Grossman-Clarke, D. Sailor, The integrated WRF/urban modelling system: development, evaluation, and applications to urban environmental problems, Int. J. Climatol. 31 (2) (2011) 273–288.
[19] H.R. Silva, R. Bhardwaj, P.E. Phelan, J.S. Golden, S. Grossman-Clarke, Development of a zero-dimensional mesoscale thermal model for urban climate, J. Appl. Meteorol. Climatol. 48 (3) (2009) 657–668.
[20] S.M. Roberts, T.R. Oke, C.S.B. Grimmond, J.A. Voogt, Comparison of four methods to estimate urban heat storage, J. Appl. Meteorol. Climatol. 45 (12) (2006) 1766–1781.
[21] V. Masson, A physically-based scheme for the urban energy budget in atmospheric models, Boundary-Layer Meteorol. 94 (3) (2000) 357–397.
[22] J. Yam, Y. Li, Z. Zheng, Nonlinear coupling between thermal mass and natural ventilation in buildings, Int. J. Heat Mass Transf. 46 (7) (2003) 1251–1264.
[23] O. Lönnqvist, On the diurnal variation of surface temperature, Tellus 14 (1) (1962) 96–101.
[24] O. Lönnqvist, Further aspects on the diurnal temperature variation at the surface of the earth, Tellus 15 (1) (1963) 75–81.
[25] A.M. Rizwan, L.Y. Dennis, L.I.U. Chunho, A review on the generation, determination and mitigation of Urban Heat Island, J. Environ. Sci. 20 (1) (2008) 120–128.
[26] R.B. Stull, An Introduction to Boundary Layer Meteorology, Kluwer Academic Publishers, 1988.
[27] J.W. Deardorff, Efficient prediction of ground surface temperature and moisture, with inclusion of a layer of vegetation, J. Geophys. Res. Oceans. 83 (1978) 1889–1903.
[28] British Standards Institution, BS 5385-2:2015: Wall and Floor Tiling. Design and Installation of External Ceramic, Natural Stone and Mosaic Wall Tiling in Normal Conditions, BSI, 2015. Code of practice.
[29] British Standards Institution, BS 7533-7:2010: Pavements Constructed with Clay, Natural Stone or Concrete Pavers. Code of Practice for the Construction of Pavements of Natural Stone Paving Units and Cobbles, and Rigid Construction with Concrete Block Paving, BSI, 2010.
[30] C. Jim, Planning strategies to overcome constraints on greenspace provision in urban Hong Kong, Town Plan. Rev. 73 (2) (2002) 127–152.
[31] M.S. Wong, J. Nichol, E. Ng, A study of the “wall effect” caused by proliferation of high-rise buildings using GIS techniques, Landsc. Urban Plan. 102 (4) (2011) 245–253.
[32] D.J. Sailor, M. Georgescu, J.M. Milne, M.A. Hart, Development of a national anthropogenic heating database with an extrapolation for international cities, Atmos. Environ. 118 (2015) 7–18.
[33] C.S.B. Grimmond, M. Blackett, M.J. Best, J. Barlow, J.J. Baik, S.E. Belcher, K. Fortuniak, The international urban energy balance models comparison project: first results from phase 1, J. Appl. Meteorol. Climatol. 49 (6) (2010) 1268–1292.
[34] A.J. Arnfield, Two decades of urban climate research: a review of turbulence, exchanges of energy and water, and the urban heat island, Int. J. Climatol. 23 (1) (2003) 1–26.
[35] J. Fenger, Urban air quality, Atmos. Environ. 33 (29) (1999) 4877–4900.